Metallurgy and materials

The beneficial effect of graphene oxide on the corrosion resistance of reinforced concrete

http://dx.doi.org/10.1590/0370-44672023770011

Danilo Oliveira do Nascimento[1,6]
https://orcid.org/0000-0002-0562-4387
Davi Ribeiro Silva[1,7]
https://orcid.org/0000-0001-8194-7412
Renato Altobelli Antunes[2,8]
https://orcid.org/0000-0003-1540-6495
Tarcizo Cruz C. Souza[3,9]
https://orcid.org/0000-0001-6437-0009
Taiza Maria Cardoso dos Reis[4,10]
https://orcid.org/0000-0002-2595-0331
Vera Rosa Capelossi[1,11]
https://orcid.org/0000-0002-0212-8388
Vanessa de Freitas Cunha Lins[5,12]
https://orcid.org/0000-0002-6357-9553

[1]Universidade Estadual de Santa Cruz – UESC, Departamento de Engenharias e Computação, Ilhéus – Bahia – Brasil.

[2]Universidade Federal do ABC - UFABC, Centro de Engenharia, Modelagem e Ciências Sociais Aplicadas, Santo André – São Paulo – Brasil.

[3]Gerdau SA - Gerdau Graphene, Departamento de Pesquisa e Desenvolvimento, São Paulo – São Paulo – Brasil.

[4]CTNano - Centro de Tecnologia em Nanomateriais e Grafeno, Belo Horizonte – Minas Gerais - Brasil.

[5]Universidade Federal de Minas Gerais – UFMG, Escola de Engenharia, Departamento de Engenharia Química, Belo Horizonte – Minas Gerais - Brasil.

E-mails: [6]dannascimento@hotmail.com, [7]daviribeiro.eng@gmail.com, [8]renato.antunes@ufabc.edu.br, [9]tarcizo.souza@gerdaugraphene.com, [10]taizacreis@gmail.com, [11]vrcapelossi@uesc.br, [12]vlins@deq.ufmg.br,

Abstract

The effect of graphene oxide (GO) on the concrete quality and the corrosion resistance of carbon steel reinforcement was evaluated. The concrete mix was calculated at a ratio of 1: 1.86: 2.14: 0.46 (cement: sand: gravel: water); the dosages of GO were 0.03 wt.% and 0.05 wt.% and the superplasticizer (PC) concentration was 0.6 wt.% concerning the cement mass. Compressive strength tests (7, 28, and 91 days), water absorption tests, determination of voids index (WATIDVI), ultrasonic pulse velocity (UPV) testing, and optical microscopy analysis were carried out. All concrete samples showed excellent compactness and low porosity. Open circuit potential measurements and linear polarization resistance (LPR) were performed during 15 cycles of partial immersion and drying of concrete in a 3.5 wt.% NaCl solution. A beneficial effect of 0.03 wt.% of GO addition on the corrosion resistance of the reinforced concrete was identified in the saline medium and the corrosion inhibition efficiency obtained was 79.3%.

Keywords: graphene oxide; corrosion; linear polarization resistance; reinforced concrete.

1. Introduction

Reinforced concrete is widely used as a structural material due to the compressive strength and the tensile and flexural strength provided by the steel reinforcement (Wu *et al*., 2019; Zeng *et al*., 2020). Even so, concrete is a porous material, which in marine environments is susceptible to the action of water and the penetration of chloride ions (Mehta and Monteiro, 2006) with the poten-tial to destroy the passive layer of steel and to generate pitting corrosion (Wright and Pantelides, 2021).

Literature reports the application of nanotechnology to improve the physical and mechanical properties of concrete (Wu *et al*., 2019). Wu *et al*. (2019) reported an improvement of the com-pressive strength of the concrete by increasing the concentration of graphene oxide (GO) nanosheets from 0.02 wt.% to 0.08 wt.% for the water–cement ratio of 0.5. GO acts by promoting the hydration process and generating the bridging effect for microcracks. Thus, GO can be beneficial for the corrosion resistance of reinforcements (Wu *et al*., 2021). The addition of 0.05% graphene oxide (GO) nanosheets (by weight of cement) improved the compressive and flexural strength of ordinary Portland cement paste by up to 58% (Pan *et al*., 2015). The mechanisms associated with improvement of the mechanical properties of cement are the interaction between the microcracks and the GO nanosheets, promotion of the hydration process, and the strong bonding between carboxylic groups and hydration products (Pan *et al*., 2015). However, most of the research is focused on the GO effect on physical and rheological properties of cement paste and cement mortar (Wu *et al*., 2019).

Concerning the corrosion resistance of reinforcements, Indukuri and Nerella (2021) reported the beneficial effect of an addition of 0.03 wt.% in cement on the durability of reinforced concrete due to reduction of chloride penetration depth. They also reported that agglomeration occurred for GO concentration above 0.03 wt.% (Indukuri and Nerella, 2021). Li *et al*. (2019) relate that when the concentration of GO approaches 0.05% in relation to the mass of the cement, the number of dispersed nanosheets reduces in the cement matrix due to stacking and the reinforcing effect of GO tends to be minimized. Ghazizadeh *et al*. (2017) state that the hydrophilic functional groups of GO are reduced when exposed to alkaline environments, which makes it difficult to disperse the nanomaterial in the cement paste. Dispersion becomes more difficult, and therefore, agglomeration increases with the increase of the GO concentration. Literature reported a reduced water absorption with a GO addition in concrete, increasing the corrosion resistance of rein-forcements (Abdalla *et al*., 2022).

Graphene oxide (GO) is a derivative of graphene, hexagonal carbon lattice with sp^2 and sp^3 hybridized orbitals, containing epoxy, carboxyl, and hydroxyl functional groups, which contribute to a hydrophilic property (Qureshi and Panesar, 2019; Qureshi *et al*., 2019). GO. In addition, cementitious materials, collaborates with the refinement of poresl, obtaining a more cohesive and resistant material (Shamsaei *et al*., 2018). GO promotes an additional formation of calcium silicate hydrated (C-S-H) (Zhao *et al*., 2020). GO sheets adsorb and immobilize calcium ions on their surface (Hou *et al*., 2019) and this phenomenon tends to form, along with C-S-H, calcium hydroxide, which contributes to the reduced porosity of the composite material (Haga *et al*., 2005), while making the material even more alkaline, enhancing steel passivation (Yamanaka *et al*., 2020). GO acts as a coating on carbon steel, increasing corrosion resistance (Yamanaka *et al*., 2020). GO acts as a type of shielding and inhibits charge transfer during the corrosion process (Liu *et al*., 2020; Arshad *et al*., 2022).

There is still a gap in literature on the effect of GO addition to cement on the corrosion of reinforcements. In addition, it is necessary to evaluate whether the range of optimal GO concen-tration described in literature, which produces an increase in mechanical properties, is also bene-ficial in the case of corrosion reinforcement. Compressive strength tests (7, 28 and 91 days), wa-ter absorption tests by immersion and determination of voids index (WATIDVI), ultrasonic pulse velocity (UPV) and optical microscopy analysis were performed. Corrosion monitoring of rein-forced concrete was carried out by using the Linear Polarization Resistance (LPR) technique dur-ing 15 cycles of partial immersion and drying in a 3.5 wt.% NaCl solution.

2. Materials and methods

Graphene oxide (GO) was provided by the Technological Center of Nanomaterials and Graphene (CTNANO) of the Federal University of Minas Gerais (UFMG), which synthesized the nanomaterial using a modification of the Hummer's method. GO was previously characterized, showing 1-7 layers, 5 µm of lateral dimension, and an oxidation degree of 40 wt.%. The materials used in the tests are Portland cement, 8 mm corrosion carbon steel rebars of type CA-50, deionized water and third generation polycarboxylate superplasticizer-PC (Li *et al*., 2021), a commercial product provided by BASF. The role of a superplasticizer in the concrete is to reduce the amount of water added to the concrete, increasing its fluidity. Other functions of the superplasticizer are: to increase workability and reduce segregation, to adjust the setting and hardening time of the concrete – either slow it down or speed it up as necessary, to increase the durability of concrete through resistance to physical actions, mechanical actions, and chemical actions, and to reduce the cost of concrete, increasing yield, facilitating placement on site, and allowing formwork to be removed in shorter periods of time. Li *et al*. (2021) reported that the dispersibility of GO together with superplasticizer in the cement matrix improves distribution and reduces the size of the cement pores, generating a more compact structure, which reduces micropores and improves the mechanical properties. Their properties provided by the manufacturers can be seen in Tables 1-4.

Table 1 - Composition of Portland cement (wt.%).

CaO	SIO_2	Al_2O_3	Fe_2O_3	MgO	K_2O	Na_2O	SO_3	Loss to fire	Insoluble residue
60.78	19.63	4.46	3.35	4.12	1.09	0.20	3.32	2.26	0.79

Table 2 - Technical specification of cement.

Initial setting time (min)	175
Final setting time (min)	265
Apparent specific mass ($g.cm^{-3}$)	1.2
Density ($g.cm^{-3}$)	2.99
Blaine ($cm^2.g$)	4.700

Table 3 - CA-50 8 mm rebar composition (wt.%).

C	Si	Mn	S	P	Cu	Ni	Cr	Sn	Nb	Mo	Fe
0.25	0.225	0.7	0.025	0.02	0.2	0.15	0.15	0.075	0.005	0.05	Bal.

Table 4 - Technical specification of polycarboxylate superplasticizer (PC).

pH	Density ($g.cm^{-3}$)	Solid content (%)	Viscosity (cps)	Recommended content (%*)
5 – 7	1.067 - 1.107	28.5 - 31.5	<150	0.2 - 1.0

*by weight of anhydrous cement.

The suspension of GO (4 $mg.L^{-1}$) was prepared by dispersing the lyophilized nanomaterial form into distilled water and PC (Table 5) for 3 hours of mixing by using a magnetic stirrer at 1,000 rpm and 2 hours of sonication at a frequency of 40 kHz (Qureshi *et al.*, 2019).

Table 5 - PC modified GO solution.

Sample	Water (mL)	GO (g)	PC (g)
GO 0.03	525	2.1	28.0
GO 0.05	875	3.5	28.0

The aggregates were characterized according to the ABNT NBR NM 248 (2003), ABNT NBR 16972 (2021), ABNT NBR 16917 (2021) and ABNT NBR 16916 (2021) standards and dried in the oven for 48 h at 100° C. The concreting was carried out according to the materials and dosages (Table 6) in the Motomil MB-150 L Concrete Mixer. After 48 hours, the specimens were demolded and immersed in a saturated solution of calcium hydroxide for the curing process, pre-scribed in the ABNT NBR 5738 (2015) standard. After 28 days, the samples were destined for the tests, being 4 samples of 10 cm x 10 cm for the compressive tests, 3 samples of 10 cm x 20 cm for the WATIDVI test, 3 samples of 10 cm x 20 cm for UPV and OM analyses, and 3 samples of 7.5 cm x 10 cm in dimension for the electrochemical tests.

Table 6 - Materials for concreting.

Sample	Water (mL)	Cement (kg)	Gravel (kg)	Sand (kg)	PC (g)	GO (g)
GO-0	3.220	7.0	15.0	13.0	42.0	-----
GO-0.03	3.220	7.0	15.0	13.0	42.0	2.1
GO-0.05	3.220	7.0	15.0	13.0	42.0	3.5

The compressive strength tests were performed by using the Emic universal machine, 2000 KN, in which the samples were broken at 7, 28 and 91 days, according to the ABNT NBR 5739 (2018) standard. The WATIDVI was performed after 28 days, according to the ABNT NBR 9778 (2005) standard.

For the UPV test, a Pundit Lab+ device with 54 kHz transducers was used and the direct method of propagation of ultrasonic waves in the longitudinal direction was applied, according to the ABNT NBR 8802 (2013) standard. The tests were carried out with the samples in a dry state, at 20° C. To corroborate the results of the UPV tests, the same samples were cut in the format of slices, with a thickness

of 1 cm and submitted to stereomicroscope analysis, using the EZ4HD Leica equipment to identify internal failures.

The steel bars were cut into 10 cm, polished using a Sander and Polisher Fortel, PLF, speed of 2 rpm, with sandpaper of 80, 220, 400 and 600 grits, and washed with distilled water, alcohol, and acetone (Zhang *et al.*, 2021). For electrical contact, copper wires with a diameter of 2.5 mm were fixed to the steel bars with insulating tape, and the steel bars were coated with the same tape, maintaining an exposed area of 6 cm², which were introduced into the concrete samples (Figure 1).

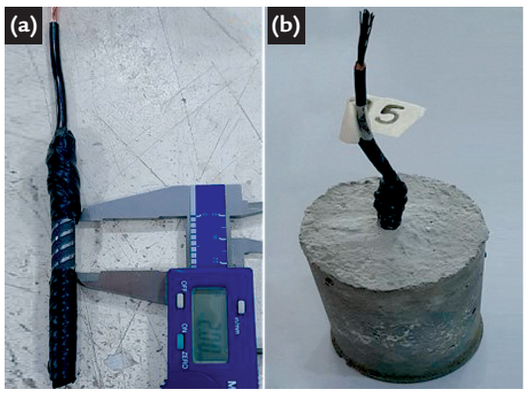

Figure 1 - (a) exposed area of the coated steel bar, and (b) reinforced concrete sample.

The reinforced concrete samples were subjected to 15 cycles of partial immersion in a 3.5 wt.% NaCl solution for 4 days, followed by drying in an oven at 60 °C for three days, simulating an aggressive environment (Alcántara *et al.*, 2017). A three-electrode electrochemical cell was used, with the AISI 304L stainless steel plate as a counter electrode, the silver/silver chloride saturated with potassium chloride as the reference electrode, and the reinforced concrete samples as the working electrode.

After measuring the open circuit potential for 60 minutes, the linear polarization resistance (LPR) technique was performed. In the LPR test, the polarization resistance (PR) was obtained using a polarization of ± 20 mV in relation to the corrosion potential (Zhang *et al.*, 2021). The equipment used was a potentiostat/galvanostat, Metrohm Autolab PGSTAT302N with NOVA 1.11 software. The scan rate was 0.667 mV/s.

3. Results and discussions

The results of aggregate characterization were shown in Table 7. The results of the aggregates characterize them as suitable and widely used materials in the production of concrete for civil construction (Silva *et al.*, 2017).

Table 7 - Characterization of aggregates.

	Gravel	Sand
Fineness module (mm)	6.40	1.98
Maximum dimension (mm)	19.00	-------
Unit mass (g/cm³)	1.55	1.59
Specific mass (g/cm³)	2.63	2.63

The results of the compressive strength, WATIDVI, UPV, and optical microscopy analysis showed no differences between samples with and without GO. In the compressive strength test, at 91 days (Figure 2) an evolution of strength of samples occurred when compared to 7 and 28 days. GO interacted with the cement matrix, contributing to the hydration process, but all samples,

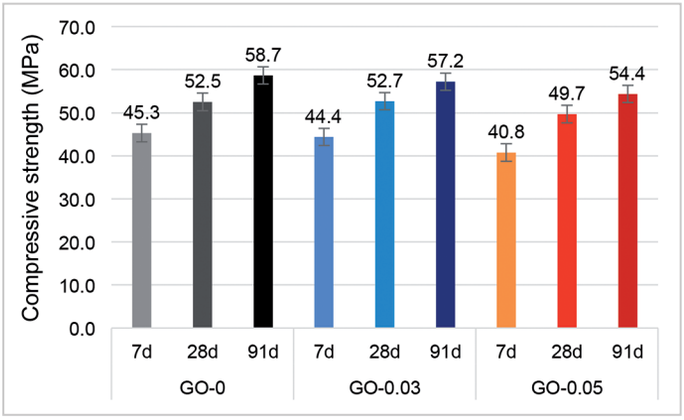

Figure 2 - Compressive strength at 7, 28 and 91 days.

with and without GO showed the same behavior (Lee *et al*., 2020). Dosages of 0.03 of GO are considered optimal for application in composite materials (Devi and Khan, 2020). GO-0.03 showed a greater similarity in compressive strength at 7, 28 and 91 days when compared to GO-0. A slight decrease in compressive resistance of GO 0.05 was observed compared to GO 0.03 and GO-0 samples, and an agglomeration of the nanomaterial may have occurred.

The results of WATIDVI (Table 8) indicate that there were no variations between the samples with and without the addition of GO, which suggests that the addition of GO in the ce-mentitious matrix did not contribute to the reduction of the concrete porosity (Du *et al*., 2016). In the UPV test, samples GO-0, GO 0.03 and GO 0.05 presented an average speed of 4,750, 4,737 and 4,701 m/s, respectively. The UPV results were superior when compared to literature (Devi and Khan, 2020). The optical micrographs (Figure 3) corroborated the UPV results, indicating that the samples showed excellent compactness and no signs of cracks were detected.

Table 8 - Water absorption (A) and voids index (Vi).

Sample	A (%)	Vi (%)
GO-0	4.57	10.86
GO 0.03	4.83	11.54
GO 0.05	4.80	11.45

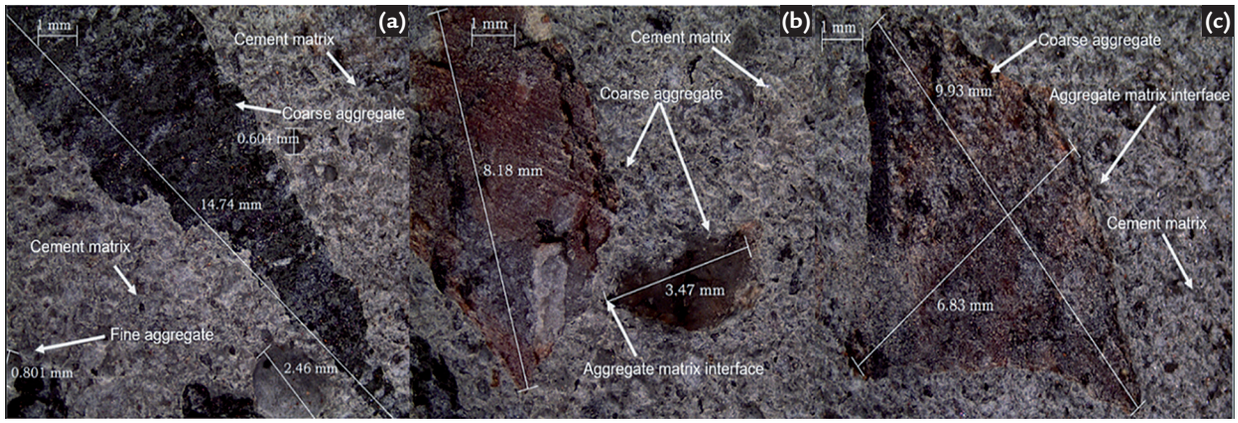

Figure 3 - Optical micrographs of (a) GO-0, (b) GO-0.03 and (c) GO-0.05.

3.1 Electrochemical evaluation

The open circuit potential (OCP) was measured for 3600 s after each cycle and the results are shown in Figure 4 for samples after 5 and 9 cycles.

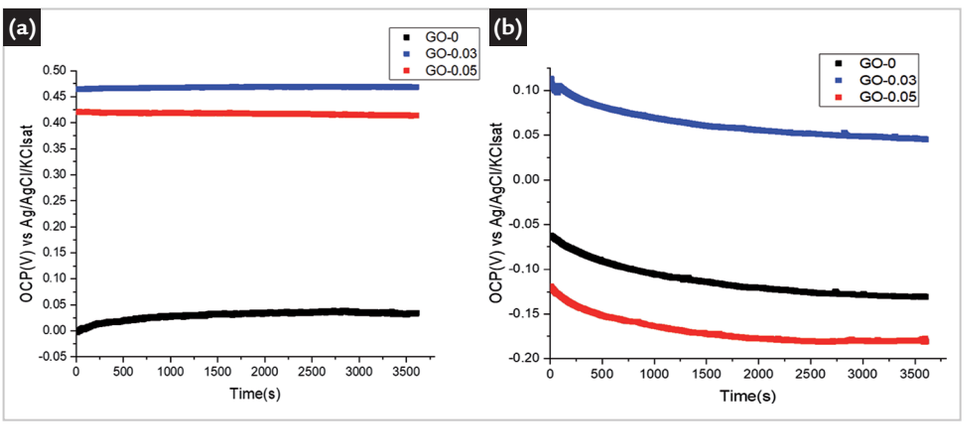

Figure 4 - Open circuit potential measurement of steel after (a) 5 cycles and (b) 9 cycles.

In the first 5 cycles, the corrosion potential (Ecorr) of the GO-0.03 and GO-0.05 rein-forced concrete samples presented a nobler behavior than the GO-0 (Table 10). In the 9th cycle, Ecorr of the GO 0.03 sample was higher than the corrosion potential of the GO-0 and GO-0.05 samples (Table 10).

The evolution of the corrosion potential over the 15 cycles of the corrosion test is shown in Figure 5. In the first 5 cycles, the Ecorr of the GO-0.03 and GO-0.05 samples showed a greater corrosion resistance when compared to GO-0. In the 7th cycle, the Ecorr of GO-0.03 and GO-0.05 were 0.23 and 0.27 V, respectively, close to that obtained by Wu *et al*. (2021). Among cycles 6 and 13, GO-0 presented higher corrosion potentials when compared to GO-0.03 and GO-0.05. In the last cycles (14° and 15°), the GO-0.03 sample presented higher Ecorr values when com-pared to GO-0 and GO-0.05. In the 15th cycle, the Ecorr values of GO-0, GO-0.03 and GO-0.05 were -0.45 V, -0.38 V and -0.40 V, respectively, which means that these samples are corroded

(Table 9). In the 15th cycle, although all samples are corroded, according to the ASTM C876-15 (2016) technical standard, GO-0 showed the least noble corrosion potential when compared to GO-0.03 and GO 0.05 (Table 9).

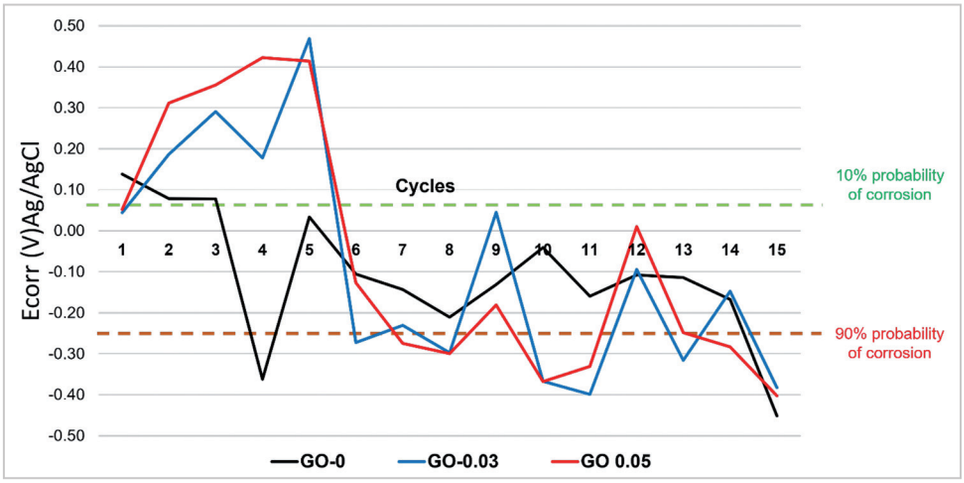

Figure 5 - Corrosion potential (Ecorr)Ag/AgCl versus drying and immersion cycles for the GO-0, GO 0.03 and GO 0.05 samples.

Table 9 - E_{corr} in cycles numbers 5, 9 and 15.

Cycle	Sample	Ecorr $(V)_{Ag/AgCl}$
5	GO-0	0.034
	GO-0.03	0.468
	GO-0.05	0.414
9	GO-0	-0.131
	GO-0.03	0.045
	GO-0.05	-0.181
15	GO-0	-0.451
	GO-0.03	-0.382
	GO-0.05	-0.403

Figure 6 shows the linear polarization curves for reinforced concrete samples in the presence of chloride ions after 13 cycles of the corrosion testing. The values of the polarization resistance obtained by calculating the slope of straight lines in the graph of potential versus current density are shown in Figures 7-9. It is interesting to note that at the beginning of the test, only the GO 0.03% sample presented a polarization resistance of the order of 10^7 Ω.cm². Afterwards, all samples show lower corrosion resistance until in the fourth and five cycles, the samples showed Rp of the order of 10^7 Ω.cm², although the GO 0.03% sample has the highest Rp value. In the sixth cycle, the sample without the addition of GO emerges as the best behavior against corrosion, with Rp of 10^5 Ω.cm². In cycle 8, it is the GO 0.03% sample that presents the highest Rp value of the order of 10^5 Ω.cm². In the last cycles, the Rp values are lower, 10^3 Ω.cm², but the GO 0.03% sample stands out with the best behavior against corrosion. The results suggest a greater corrosion re-sistance of the GO 0.03 sample and, consequently, a beneficial action of GO, at very low doses, in the protection of carbon steel in reinforced concrete in saline environments (Razavizadeh and Ghorbani, 2019).

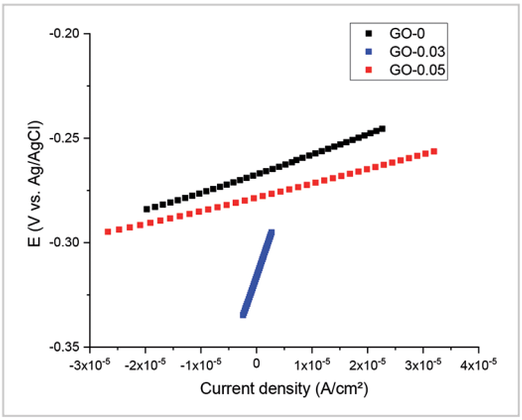

Figure 6 - Linear polarization curves for reinforced concrete samples in the presence of chloride ions after 13 cycles of corrosion test.

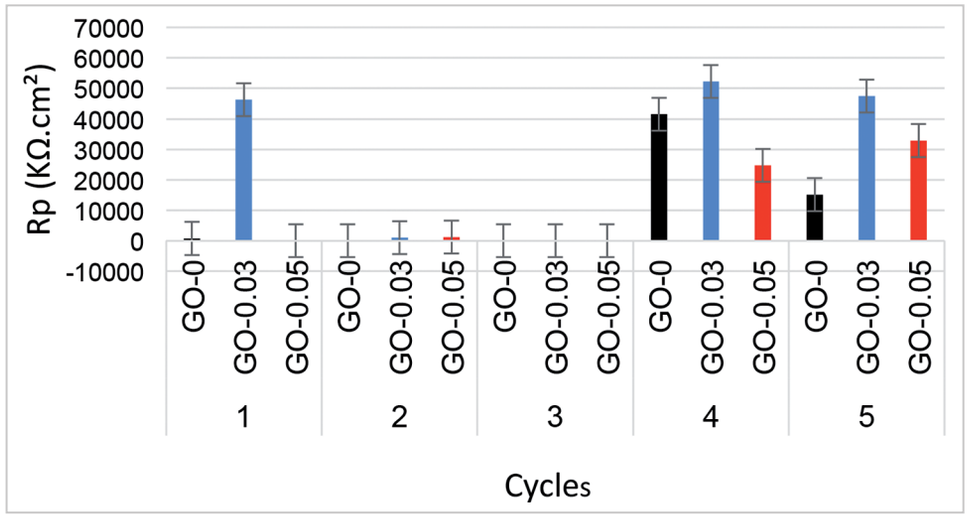

Figure 7 - Polarization resistance values for reinforced concrete samples in the presence of chloride ions - cycles 1 to 5.

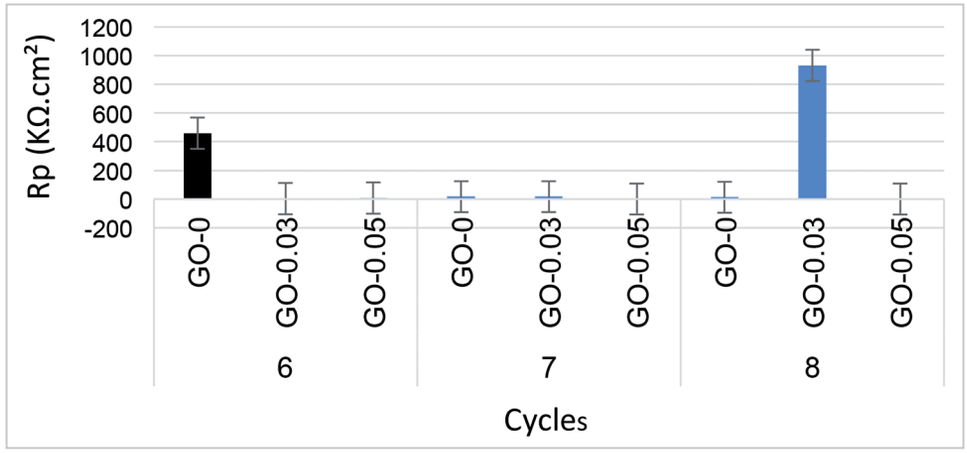

Figure 8 - Polarization resistance values for reinforced concrete samples in the presence of chloride ions - cycles 6 to 8.

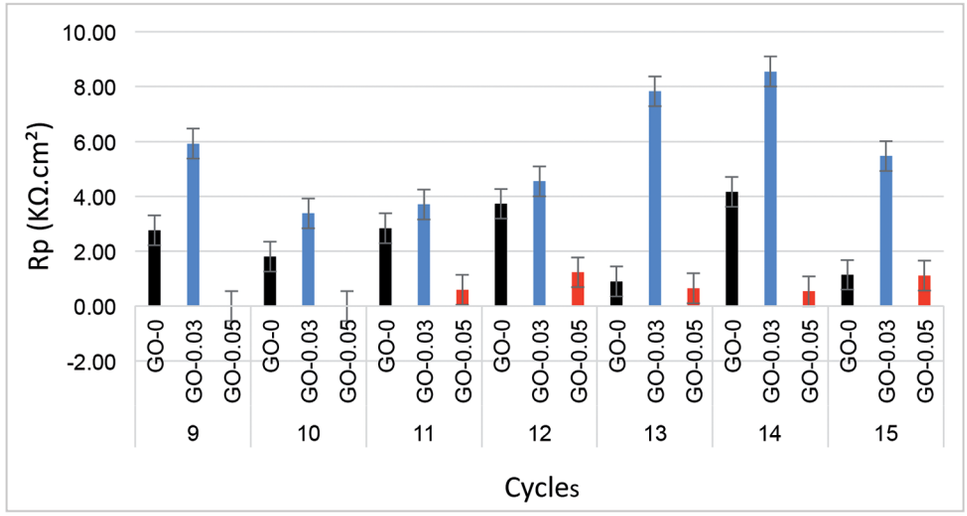

Figure 9 - Polarization resistance values for reinforced concrete samples in the presence of chloride ions - cycles 9 to 15.

The beneficial effect of GO improving the corrosion resistance of steel reinforcements is clear, mainly after the last cycles. After 15 cycles of the corrosion test, the inhibition efficiency for the 0.03 wt.% GO addition in concrete is 79.3%. The addition of 0.05 wt.% of GO in relation to the cement mass did not increase the polarization resistance of carbon steel in concrete containing chlorides, after 15 cycles of the corrosion test.

After 15 cycles of corrosion test, the GO 0.03 sample showed a Rp value of 5.5 kΩ.cm², 23.6% higher than that found by Zhu and Zhang (2021) of 4.2 kΩ.cm². The mechanisms involved are the adsorption of calcium ions on the GO surface (Hou *et al.*, 2019) and this phenomenon tends to form, along with C-S-H, calcium hydroxide, which contributes to a higher alkalinity of the composite material (Haga *et al.*, 2005), enhancing the steel passivation (Yamanaka *et al.*, 2020). GO acts as a coating on carbon steel increasing corrosion resistance (Yamanaka *et al.*, 2020). GO acts as a type of shielding and

inhibits charge transfer during the corrosion process (Liu *et al*., 2020; Arshad *et al*., 2022). Silva *et al*. (2023) identified an anticorrosion mechanism of the GO in the cement extract containing chlorides by XPS analysis. The nanomaterial caused an increase in the hematite/magnetite ratio. The Fe_2O_3 is more stable than Fe_3O_4 in the passive layer. The addition of the nanomaterial in the system formed a more protective passive layer on the metallic surface, improving its stability.

4. Conclusions

The GO 0.03 wt.% addition in the concrete did not affect the compressive strength of samples. There was a slight decrease in compressive strength for the GO-0.05 sample, at 7, 28 and 91 days when compared to GO-0.

The GO addition did not decrease the porosity of the composite material. All samples showed excellent compactness and did not present failures and cracks visible by optical microscopy and detectable by ultrasonic pulse velocity testing.

After 15 cycles of the corrosion test, the corrosion potential of the sample with 0.03 wt.% GO addition was higher than the Ecorr of the samples without GO and with 0.05 wt.% GO.

After 15 cycles, the GO 0.03 sample presented higher polarization resistance values when com-pared with the GO-0 and GO 0.05 samples.

After the 15th cycle, the polarization resistance of the GO 0.03 was 5.5 kΩ.cm², while the po-larization resistance values of the reference sample and the GO 0.05 sample were 1.1 kΩ.cm². The corrosion inhibition efficiency of addition of 0.03 wt.% in relation to the cement mass was 79.3%.

Acknowledgments

The authors thank the financial support of Conselho de Desenvolvimento Científico e Tecnológi-co (CNPq), grant number 306291/2018-5.

References

ABDALLA, J. A.; THOMAS, B. S.; HAWILEH, R. A.; SYED, K. I.; KABEER, A. Influence of nanomaterials on the water absorption and chloride penetration of cement-based concrete. ***Materials Today: Proceedings,*** v. 65, p. 2066-2069, 2022.

ALCÁNTARA, J.; DE LA FUENTE, D.; CHICO, B.; SIMANCAS, J.; DÍAZ, I.; MORCILLO, M. Marine atmospheric corrosion of carbon steel: a review. ***Materials,*** v. 10, p. 406, 2017.

ARSHAD, M. U.; DUTTA, D.; SIN, Y. Y.; HSIAO, S. W.; WU, C. Y.; CHANG, B. K.; DAI, L.; SU, C. Y. Multi-functionalized fluorinated graphene composite coating for achieving durable electronics: ultralow corrosion rate and high electrical insulating passivation. ***Carbon,*** v. 195, p. 141-153, 2022.

DEVI, S. C.; KHAN, R. A. Effect of graphene oxide on mechanical and durability performance of concrete. ***Journal of Building Engineering,*** v. 27, 101007, 2020.

DU, H.; GAO, H. J.; PANG, S. D. Improvement in concrete resistance against water and chloride ingress by adding graphene nanoplatelet. ***Cement and Concrete Research,*** v. 83, p. 114–123, 2016.

GHAZIZADEH, S.; DUFFOUR, P.; SKIPPER, N. T.; BILLING, M.; BAI, Y. An investigation into the colloidal stability of graphene oxide nano-layers in alite paste. ***Cement and Concrete Research,*** v. 99, 2017.

HAGA, K.; SUTOU, S.; HIRONAGA, M.; TANAKA, S.; NAGASAKI, S. Effects of porosity on leaching of Ca from hardened ordinary Portland cement paste. ***Cement and Concrete Research,*** v. 35, p. 1764-1775, 2005.

HOU, D.; ZHANG, Q.; WANG, M.; ZHANG, J.; WANG, P.; GE, Y. Molecular dynamics study onwater and ions on the surface of graphene oxide sheet: effects of functional groups. ***Computational Materials Science,*** v. 167, p. 237–247, 2019.

INDUKURI, C. S. R.; NERELLA, R. Enhanced transport properties of graphene oxide based cement composite material. ***Journal of Building Engineering,*** v. 37,102174, 2021.

LEE, S.; JEONG, S.; KIM, D.; WON, J. Graphene oxide as an additive to enhance the strength of cementitious composites. ***Composite Structures,*** v. 242, 112154, 2020.

LI, C. Y.; CHEN, S. J.; LI, W. G.; LI, X. Y.; RUAN, D.; DUAN, W. H. Dynamic increased reinforcing effect of graphene oxide on cementitious nanocomposite. ***Construction and Building Materials,*** v. 206, p. 694-702, 2019.

LI, Q.; HE, C.; ZHOU, H.; XIE, Z.; LI, D. Effects of polycarboxylate superplasticizer-modified graphene oxide on hydration characteristics and mechanical behavior of cement. ***Construction and Building Materials,*** v. 272, 2021.

LIU, Q.; ZHANG, X.; ZHOU, W.; MA, R.; DU, A.; FAN, Y.; ZHAO, X.; CAO, X. Improved anti-corrosion behaviour of an inorganic passive film on hot-dip galvanised steel by modified graphene oxide incorporation. ***Corrosion Science,*** v. 174, 108846, 2020.

MEHTA, P. K.; MONTEIRO, P. J. M. ***Concrete***: microstructure, properties, and materials. McGraw-Hill, 2006.

PAN, Z.; HE, L.; QIU, L.; KORAYEM, A. H.; LI, G.; ZHU, J. W.; COLLINS, F.; LI, D.; DUAN, W. H.; WANG, M. C. Mechanical properties and microstructure of a graphene oxide-cement composite. ***Cement and Concrete Composites,*** v. 58, p. 140-147, 2015.

QURESHI, T. S.; D. K. PANESAR, D. K. Impact of graphene oxide and highly reduced graphene oxide on cement based composites. ***Construction and Building Materials,*** v. 206, p. 71-83, 2019.

QURESHI, T. S.; PANESAR, D. K.; SIDHUREDDY, B.; CHEN, A.; WOOD, P. C. Nano-cement composite with graphene oxide produced from epigenetic graphite deposit. ***Composites Part B***: Engineering, v. 159, p. 248-258, 2019.

RAZAVIZADEH, O.; GHORBANI, M. Surface modification of carbon steel by ZnO-graphene nano-hybrid thin film. ***Surface and Coatings Technology,*** v. 363, 1-11, 2019.

SHAMSAEI, E.; SOUZA, F. B.; YAO, X.; BENHELAL, E.; AKBARI, A.; DUAN, W. Graphene-based nanosheets for stronger and more durable concrete: a review. ***Construction and Building Materials,*** v. 183, p. 642-660, 2018.

SILVA, D. R. ***Estudo da potencialidade do óxido de grafeno como aditivo inibidor da corrosão do aço carbono CA-50 em matriz cimentícia contendo cloretos,*** Dissertação (Mestrado) - Universidade Estadual de Santa Cruz, Ilhéus, BA, 2022.

SILVA, D. R.; NASCIMENTO, D. O.; ANTUNES, R. A.; SOUZA, T. C. C.; REIS, T. M. C.; CISQUINI, P.; CAPELOSSI, V. R.; LINS, V. F. C. Graphene oxide as a corrosion inhibitor for steel reinforcement in cement extract containing chlorides. ***Journal of Materials Engineering and Performance,*** p. 1-10, 2023.

SILVA, M. A.; PEPE, M.; ANDRADE, R. G. M.; PFEIL, M. S.; TOLEDO FILHO, R .D. Rheological and mechanical behavior of high strength steel fiber-river gravel self compacting concrete. ***Construction and Building Materials,*** v. 150, p. 606-618, 2017.

WRIGHT, J. W.; PANTELIDES, C. P. Axial compression capacity of concrete columns reinforced with corrosion-resistant hybrid reinforcement. ***Construction and Building Materials***, v. 302, 124209, 2021.

WU, W.; CHEN, R.; YANG, Z.; HE, Z.; ZHOU, Y.; LV, F. Corrosion resistance of 45 car-bon steel enhanced by laser graphene-based coating. ***Diamond & Related Materials,*** v. 116, 2021.

WU, Y. Y.; QUE, L.; CUI, Z.; LAMBERT, P. Physical properties of concrete containing graphene oxide nanosheets. ***Materials,*** v. 12, p. 1707, 2019.

YAMANAKA, S.; HIRANO, S.; UWAI, K.; TOKURAKU, K. Design of calcium hydroxide–based granules for livestock sanitation. ***Case Studies in Chemical and Environmental Engineering,*** v. 2, 100005, 2020.

ZENG, M. H.; WU, Z. M.; WANG, Y. J. A stochastic model considering heterogeneity and crack propagation in concrete. ***Construction and Building Materials,*** v. 254, 119289, 2020.

ZHANG, L.; NIU, D.; WEN, B.; FU, Q.; PENG, G.; SU, L.; BLACKWOOD, D. J. Initial-corrosion condition behavior of the Cr and Al alloy steel bars in coral concrete for marine construction. ***Cement and Concrete Composites,*** v. 120, 104051, 2021.

ZHAO, L.; GUO, X.; SONG, L.; SONG, Y.; DAI, G.; LIU, J. An intensive review on the role of graphene oxide in cement-based materials. ***Construction and Building Materials,*** v. 241, 117939, 2020.

ZHENG, Z. J.; GAO, Y.; GUI, Y.; ZHU, M. Studying the fine microstructure of the passive film on nanocrystalline 304 stainless steel by EIs, XPS and AFM. ***Journal of Solid State Electrochemistry,*** v. 18, p. 2201-2210, 2014.

ZHU, Y.; ZHANG, Z. Investigation of the anticorrosion layer of reinforced steel based on graphene oxide in simulated concrete pore solution with 3 wt% NaCl. ***Journal of Building Engineering,*** v. 44, 103302, 2021.

Received: 13 February 2023 - Accepted: 26 February 2024.